Optica Applicata, Vol. XXXV, No. 4, 2005

Photostimulated defect formation in gel-derived biomaterial

STANISŁAWA SZARSKA[1], AGATA WÓJCIK[2]

[1]Institute of Physics, Wrocław University of Technology, Wybrzeże Wyspiańskiego 27, 50-370 Wrocław, Poland

[2]Institute of Physics, University of Zielona Góra, ul. prof. Szafrana 4a, 65-516 Zielona Góra, Poland

Intensive research in the field of biomaterials proved that introducing bone implants to a human body causes a modification of an electric field connected with the bone surface. It is possible that this may be, to a great extend, the cause of an adverse reaction of the body to the implant. The surface of implant materials may be highly variable depending on the preparation procedure and external agents. The aim of the investigation was to confirm the porosity of the biomaterials (gel glasses, corundum and cement), using a scanning and optical microscope, and thermoluminescence. The charge transfer was measured by a photo-stimulated exoemission method. The measurement results prove a high sensitivity of our experimental method to the effects of the surface glass modifications. Moreover, the results of our measurements allow preliminary identification of the transport mechanism in the material under consideration.

Keywords: bio-gel, biomaterials, exoelectron emission.

1. Introduction

It is well recognized that understanding the nature of biomaterial surface is essential both for understanding the interactions between materials and living systems and for fabrication of biomaterials and biomedical devices. Some of these materials possess much higher moduli than those of bone, some have not good mechanical properties. If an implant which is stiffer than bone is placed in this bone, the latter will be subjected to a reduced mechanical load and will hence resorb. It was therefore reasonable to combine a two materials to produce a composite which would match bone, both mechanically and biologically. The future of biomaterials lies in composites, since they have good mechanical properties and their surface layer is bioactive. A characteristic feature common to bioactive materials is that they bond to human bone with no fibrous tissue at the interface. At present, bioactive materials include some calcium phosphate compounds, melt and sol-gel-derived bioactive glasses, bioactive glass-ceramics and composites containing bioactive phase. In bioactivity, the essential condition for bioactive glasses to bond to living bone is the formation of a certain type of biologically active apatite layer (hydroxyapatite – HA) on their surface [1]. This is associated with

the surface characteristics of sol-gel glasses, such as their large surface areas and porous textures. Although the influence of the surface structure on HA formation is still not fully understood, several hypotheses have been suggested, based on effects of surface charge, texture (pore size and pore volume), and surface hydroxyl group [2–4]. If the resulting pores and interconnecting channels are of appropriate size, rapid bone ingrowths will occur, assuming appropriate conditions during tissue healing. These include the general requirements of adequate blood supply and osteogenetic potential of host tissues [5].

The interaction of wide gap solids with ionizing radiation results in three known defect-related events: excitation of the electronic system, primary creation of free charge carriers, electron-hole pairs as well as excitons, and creation or structure modification of defects. Some of the charge carriers are captured after external stimulation by glass matrix defects and the glass is thus transferred into a non-equilibrium state. Subsequent optical and mechanical treatments lead to defect-related relaxation processes, which are manifested in a variety of optical, electrical, magnetic and other phenomena [6].

Introducing the bone implants in a human body leads to modifications of the electric charge connected with the bone surface [7]. It is possible that changes of surface charge caused by mechanical deformation may considerably enhance the adverse reaction to this implant by the body. The last investigations [8–10] indicate that the problem of mechanism of stress-generated surface charge upon mechanical deformation is not completely understood. Different views on the source of surface charge still exist. Probably the bioelectrical potentials are involved in the generation, repairing and re-modelling of a bone tissue. Damage to materials provoke emission of negative and positive particles. Emission of each particle is related to destruction of an atomic/molecular single bond. Thus, the emission current is directly proportional to the number of bonds being broken. These broken bonds exist initially in thermodynamically non-equilibrium state. This condition leads to relaxation of broken bonds. The liberated energy may also be spent in emission of particles. In such a case, the number of particles is directly proportional to the number of relaxed broken bonds. The phenomenon under consideration is usually referred to as exoemission (EE). Studying its kinetics, one can explore both the early stages of damage and the following relaxation of the material [11]. Mechanical deformation and fracture of biomaterials, emission of energetic electrons, ions, and neutral particles is observed. This phenomenon is called fracto-emission [12]. The surface charge was investigated by optical stimulated exoelectron emission (OSEE).

Results of luminescence and electron emission measurements after irradiation of a set of biomaterials are discussed in terms of the kind of defects in the glass structure.

2. Experimental procedures

In agreement with an earlier investigation [13, 14] three types of biogel glasses of the nominal composition of 36% CaO, 60% SiO_2, 4% P_2O_5 (molar percentage), were obtained. The sol-gel precursors used in this study were tetraethoxysilane (TEOS,

$Si(OC_2H_5)_4$), calcium nitrate tetrahydrate ($Ca(NO_3)_2{\cdot}4H_2O$) dissolved in distilled water, triethylphosphate (TEP, $OP(C_2H_5O)_3$), ethanol (C_2H_5OH) as organic solvent, hydrochloric acid (HCl) as a catalyst of the reaction of hydrolysis.

The volume ratio of $TEOS:C_2H_5OH:HCl$ was 10:20:0.04 (4b sample), 10.2:11.53:0.48 (L sample), or 10.9:12.35:0.5 (K and M + water sample). Initially, the procedure involved preparing the sol-gel by mixting distilled water, appropriate alkoxide precursors and salts, and the catalyst for hydrolysis, HCl. After mixing the alkoxide components for 2 hours, the sol was cast into containers and loosely covered. Applying a spin-coating method, coated k9 glass substrate gelations were obtained. Then these films were pulled out from gel and aged at room temperature for 3–6 weeks. After that, the samples were put into an oven at 120°C for 7 days. The dried gels were heated in air at a rate of 5°C/min up to 450°C and kept in this temperature for about 1 h.

Also other biomaterials were examined:

1. Al_2O_3: granulation: I (big grains) 0.8–5 mm, II (medium grains) 0.25–0.8 mm, III (small grains) smaller than 0.3 mm [15];
2. Cement: CaO – 50.8%, Al_2O_3 – 14.8%; SiO_2 – 17.4%; SO_3 – 16.9% [16].

Microstructure of these samples was examined by optical microscopy and SEM (model JSM-5800LV JEOL, Japan). Thermoluminescence (TL) measurements were preformed on a revised Risø TL/OSL-DA-12 automated reader [18]. A 20 mCi Sr-90 source of irradiation was used. When measuring thermally stimulated processes, the linear heating rate was 1°C/s.

The OSEE current was registered by a secondary electron multiplier (10^{-18} A) in vacuum chamber with 10^{-4} Pa. Measurements of optical-stimulated kinetics were carried out using interference filters. This method has been described elsewhere [17].

3. Result and discussion

Obviously the properties of the microstructure of ceramic materials (glasses are their subclasses) are strongly related to the used processing routes. In particular, the grain size and grain size distribution, nature of grain boundaries and pore structure are very important parameters.

3.1. Surface image

Optical microscope and SEM images in Figs. 1and 2 demonstrate the porous structure of bioglass and corundum surface. Analysis of these images shows the sizes of pores to be quite different in different biomaterials.

The sizes of pores of corundum (in μm) were: 1000 – 10.1%, 800 – 13.5%, 500 – 15.2%, 300 – 22.2%, 200 – 16.9%, 100 – 22.1%.

The Table presents the sizes of pores for different types of bioglass. The biggest pores have been found for corundum samples. The size of pores for 4b film on corundum is almost homogeneous. The texture was very sensitive to technological conditions. Smaller pore diameters were obtained when the relative humidity was

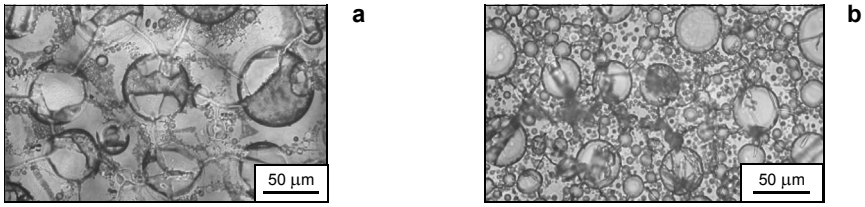

Fig. 1. Optical microscopic image of: M bioglass film sample (**a**), L bioglass film sample (**b**).

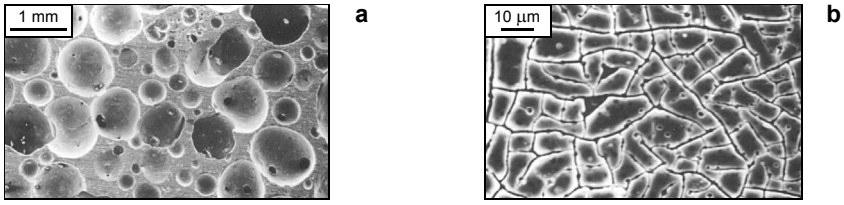

Fig. 2. SEM image of: porous corundum ceramic (**a**), 4b bioglass film on corundum (**b**).

T a b l e. Textural characteristic of bioactive glass.

Pores size [μm]		50	30	25	18	10	5	2	1
Bioglass	L	—	0.70%	3%	1.30%	11%	10.30%	—	73.70%
	M	12%	—	—	—	6%	82%	—	—
	4b	—	—	—	—	—	—	100%	—

decreased. The elastic properties of ceramics determine their mechanical behaviour and elastic constants are also strongly dependent on the microstructure. In particular, porosity has a significant effect on elastic constant, which decreases with increasing pore content. Besides pore content, pore shape and pore orientation also affect the elastic behaviour of ceramics and glasses. If porous corundum (inert ceramic) implants have pores with diameters above 100 μm, bone ingrowth may occur, which anchors the bone to the material (biological fixation). The potential advantage offered by porous corundum is the mechanical stability of the bone-implant interface that develops when bone grows into the pores. Lower mechanical strength and brittleness are the disadvantages associated with porous corundum implants. In the case of bioglasses, the materials are attached directly by chemical bonding to the bone (bioactive fixation) and the diameter of the pores could be smaller. The attachment and bonding of inert corundum implant to bone can be enhanced by using bioactive glasses as coatings. In our opinion, the best composition of bioactive coatings is M composition, because 4b composition has too small pores and L composition reveals the diameters of the pores to vary too much.

3.2. Luminescence investigation

Typical glow curves for 2 Gy irradiated biomaterials exposed to gamma rays are presented in Figs. 3 and 4.

TL glow curves for the bioglass film and biogel glass powder irradiated with a dose of 2 Gy are presented in Fig. 3. For the powdered biogel we observed a first maximum at about 120°C, and an increase in luminescence above 350°C. After the first heating of these samples to 300°C, the 120°C maximum disappeared. The first TL maximum for the thin film of biogel is shifted to 240°C.

Earlier ESR and TL investigations of bioglasses, the basic composition of which was close to that of biogel, indicate that heating at 110–120°C leads to generation of stable paramagnetic hole centers [19].

The TL emission from corundum without excitation was weak and the glow curves showed no maxima. In Fig. 4**a** typical glow curves for different granulation of 2 Gy irradiated samples are presented. The TL curve, which was obtained for an γ-irradiated

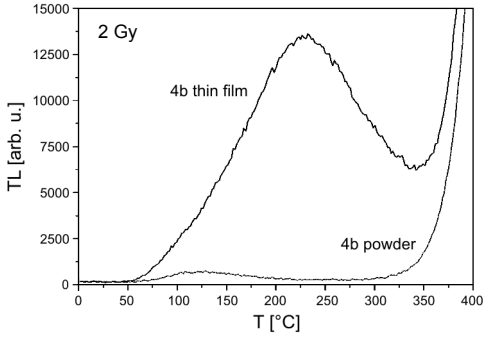

Fig. 3. TL glow curves for 4b biogel samples.

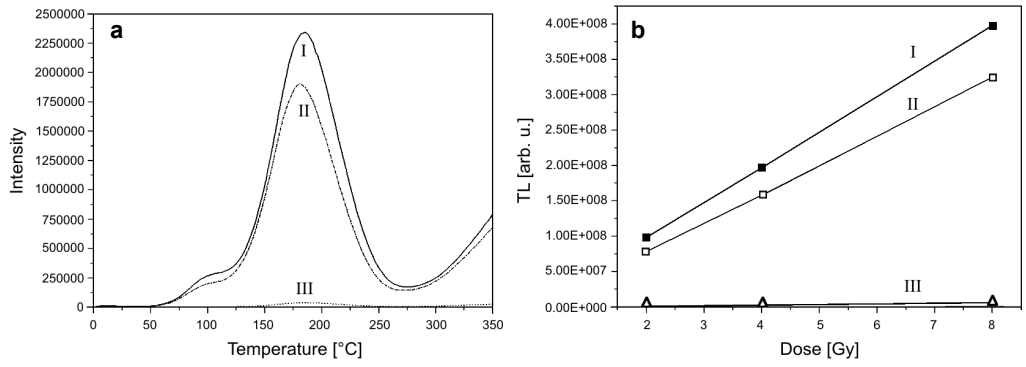

Fig. 4. TL glow curves for granulated corundum: I – big grains, II – medium grains, III – small grains (**a**), the dose dependence of 190°C maximum (**b**).

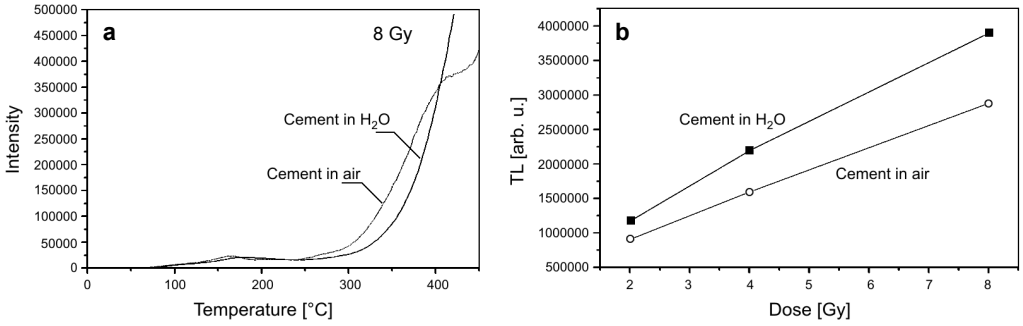

Fig. 5. TL glow curves for two types of preparation of 8 Gy irradiated cement samples (**a**), the dose dependence of the 165°C (cement in air) and 185°C (cement in H_2O) maximum (**b**)

sample, was dominated by one peak with a maximum near 190°C (460 K) for big grains (I), 180°C (450 K) for medium (II) grains, and a broad small maximum for the smallest (III) grains. Surdo obtained 450 K TL peak for crystalline Al_2O_3. The parameters of this peak, such as temperature of the peak maximum, and the kinetics order, suggest the electronic origin of the trap, which absorbs at 2.8 eV and is emptied near 450 K [20]. A defective aluminium oxide with strong oxygen nonstoichiometry, which consists in high concentration of one F^+- and two F-electron vacancy centers, is critical for storing the dosimetric information. The difference of the dose dependence (Fig. 4**b**) indicates that the concentration of F-defect is dependent of a grain sizes. The photostimulated $F \rightarrow F^+$ conversion leads to both a considerable increase in the sensitivity of corundum and qualitative change in TL of the main dosimetric trap. However, issues that remain unclear so far include the release of electrons from the trap, which is emptied at 190°C, and the mechanism of the F-center luminescence excitation. Carriers may be released from these traps not only through the thermally activated and tunneling processes, but also thanks to the Auger process.

In Figures 5**a** and **b**, typical glow curves and dose dependences for differently prepared 8 Gy irradiated cement samples are presented. For both types of preparation of the cement samples we observed a first maximum in different places. For cement in air we observe TL maximum at 165°C, and an increase in luminescence above 350°C. For cement in water TL maximum is shifted to 185°C.

Comparing the luminescence signals of biogel glass samples being differently prepared and cements containing calcium silicates, phosphates and borates indicates that the efficiency for generation and type of radiation-induced centers strongly depends on the composition of the biomaterial and the way the sample is prepared.

3.3. Photostimulated electron emission

In Figures 6 and 7 we observe a decay curve of exoelectron emission from porous corundum without and with biogel glass film and cement, respectively. Surface of a aluminium oxide is well known and a stable source of exoelectrons. The time of

emptying electron traps of bioglass film is longer than that for cement sample traps (compare Figs. 6**b** and 7).

The assumed interrelation between EE and migration cation vacancies can be explained as follows: when the cation vacancy meets a divalent ion (for instance, O^{-2}), they can interact with each other, resulting in the formation of dipole. Since the cation vacancy has a negative effective charge, in order to preserve the local electrical neutrality, an electron with energy of dipole formation must leave the local region. It can also be emitted from the glass due to the accelerating action of the radiation -inducing field. This example is not the only possibility of electron releasing. In various cases, depending upon the state of the sample structure, different processes can be observed. In the case of modified biomaterial surface the different processes can be the sources of electrons. Many dangling bonds and charged defect centers can be created by bond breaking in the fracture zone, the mosaic charge distribution can cause local electric field, which can accelerate the unstable electrons to emit from the fracture zone. The charged surface may be either positive or negative, depending on the

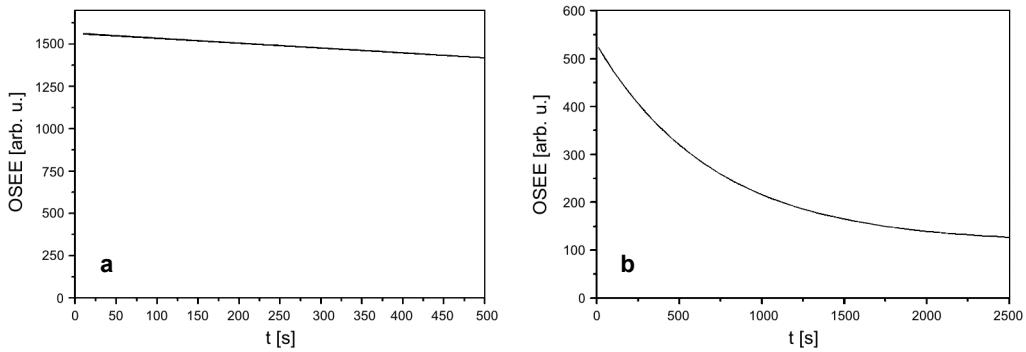

Fig. 6. Decay curve of optically stimulated electron emission in the case of 257 nm stimulated light from porous corundum without (**a**) and with (**b**) biogel film.

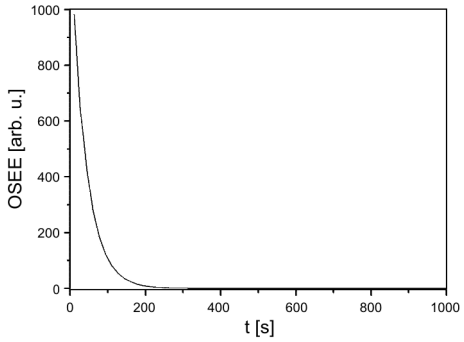

Fig. 7. Decay curve of optically stimulated electron emission in the case of 225 nm stimulated light from cement.

biomaterial composition. In the case of bioglass film on corundum, the higher negative electric potential on the surface indicates larger concentration of cations in the electric double layer on surface than that of the cement sample.

4. Conclusions

Comparison of the TL signal for both types of biogel glasses and cement samples shows that the efficiency for generation and type of radiation-induced defects strongly depends on the sample preparation.

Termoluminescence and exoemission methods are sensitive to the fine surface changes of biomaterials submitted to the action of external factors (UV, γ-ray irradiation).

The occurrence of electron discharges in the biogel sample is caused by the accumulation of surface charge and contamination of the surface. Studies of the influence of external factors on electric charge formation and its liberation are of great importance, because in many cases the charge accumulation and further breakdowns leading to mechanical destruction of insulating material precede the irreversible changes. In the case of all of these materials there is a simultaneous separation or recombination of charges that brings about a pulse fluctuation of emission current.

References

[1] HENCH L.L., *Biomaterials: a forecast for the future*, Biomaterials **19**(16), 1998, pp. 1419–23.
[2] JONES J., SEPULVEDA P., HENCH L.L., *Dose-dependent behavior of bioactive glass dissolution*, Journal of Biomedical Materials Research Part B: Applied Biomaterials **58**(6), 2001, pp. 720–6.
[3] SHI D., *Biomaterials and Tissue Engineering*, Springer, Berlin 2004.
[4] BORSOWSKA A., SZARSKA S., JASIORSKI M., MARUSZEWSKI K., STRĘK W., *Optical and structural properties of sol-gel derived bioactive glasses*, Optica Applicata **33**(1), 2003, pp. 107–14.
[5] PILLIAR R.R., *Implant surface design for development and maintenance of osseointegration*, [In] *Bio-Implant Interface: Improving Biomaterials and Tissue Reactions*, [Eds.] J.E. Ellingsen, S.P. Lyngstadaas, CRC Press, 2003, p. 43.
[6] TALE I., *Optical and magnetic resonance spectroscopy of stimulated recombination processes in defect studies*, Radiation Measurements **38**(4-6), 2004, pp. 639–44.
[7] LI P., ZHANG F., *The electrochemistry of a glass surface and its application to bioactive glass in solution*, Journal of Non-Crystalline Solids **119**(1), 1990, pp. 112–8.
[8] HENCH L.L., JONES J.R. [Eds.], *Biomaterials, Artifical Organs and Tissue Engineering*, Woodhead Publishing Limited, Cambridge, England 2005.
[9] DEKHTYAR YU., KAWAGUCHI Y., ARNAUTOV A., *Failure and relaxations of carbon fibre-reinforced plastic tested by exoemission and luminescence methods*, International Journal of Adhesion and Adhesives **17**(1), 1997, pp. 75–8.
[10] LANGFORD S.C., DICKINSON J.T., JENSEN L.C., PEDERSON L.R., *Positive-ion emission from the fracture of fused silica*, Journal of Vacuum Science and Technology A: Vacuum, Surfaces, and Films **7**(3), 1989, pp. 1829–34.
[11] KAWAGUCHI Y., *Time-resolved fractoluminescence spectra of silica glass in a vacuum and nitrogen atmosphere*, Physical Review B: Condensed Matter **52**(13), 1995, pp. 9224–8.

[12] KAWAGUCHI Y., *OH-content dependence of fractoluminescence spectra in silica glass*, Physical Review B: Condensed Matter **54**(14), 1996, pp. 9721–5.
[13] ŁĄCZKA M., JAEGERMANN Z., CHOLEWA K., CIOŁEK L., *Pokrywanie porowatych implantów korundowych warstwami szkieł bioaktywnych metodą zol-żel*, Szkło i Ceramika **1**, 1996, pp. 14–9 (in Polish)
[14] PEREIRA M.M., CLARK A.E., HENCH L.L., *Calcium phosphate formation on sol-gel-derived bioactive glasses in vitro*, Journal of Biomedical Materials Research **28**(6), 1994, pp. 693–8.
[15] ROSIEK G., MIKSIEWICZ C., BIENIEK J., *Properties of the bone-porous biomaterials*, Szkło i Ceramika **25**, 1984, pp. 41–4 (in Polish).
[16] WALA D., ROSIEK G., *Fast-setting belite-sulphoaluminate cement for special applications*, Cement, Wapno, Beton, No. 2, 2001, pp. 60–4 (in Polish).
[17] SZARSKA S., MAGIERSKI W., *OSEE as the method of determining of defect degree for a fibre preforms*, Proceedings of the SPIE **670**, 1986, pp. 109–11.
[18] BOTTER-JENSEN L., ANDERSON C.E., DULLER G.A.T., MURRAY A.S., *Developments in radiation, stimulation and observation facilities in luminescence measurements*, Radiation Measurements **37**(4-5), 2003, pp. 535–41.
[19] PADLYAK B., SZARSKA S., JUNGNER H., *Radiation-induced paramagnetic centers in Bioglass®*, Optica Applicata **30**(4), 2000, pp. 709–17.
[20] SURDO A.I., KORTOV V.S., *Exciton mechanism of energy transfer to F-centers in dosimetric corundum crystals*, Radiation Measurements **38**(4-6), 2004, pp. 667–71.

Received October 3, 2005